frontiers in Materials

ORIGINAL RESEARCH
published: 17 November 2021
doi: 10.3389/fmats.2021.769579

Tensile Behavior of Hybrid Fiber-Reinforced Ultra-High-Performance Concrete

*Jiayue Li and Zongcai Deng**

The Key Laboratory of Urban Security and Disaster Engineering, Ministry of Education, Beijing University of Technology, Beijing, China

Thirty dog bone-shaped specimens were tested to study the effects of steel fiber mixed with seven kinds of non-metallic fibers on the tensile properties of ultra-high-performance concrete (UHPC). Through experiments and micromorphological analysis, the effects of hybrid fibers on the compressive strength, tensile strength, peak strain, fracture energy, and characteristic length of UHPC were analyzed. The results showed that the hybrid fiber-reinforced UHPC showed good ductile failure characteristics, which reflected the good crack resistance and toughening effect of different fibers. The tensile stress–strain curves of UHPC with different hybrid fibers can be divided into two parts: ascending section and softening section, and the softening section was greatly affected by the type and content of fibers. Basalt fiber with a diameter of 0.02 mm had the most obvious strengthening effect on UHPC, and polyvinyl alcohol fiber with a diameter of 0.2 mm and length of 8 mm had the best toughening effect. The mixing of steel fiber and non-metallic fiber cannot only reduce the preparation cost but also improve the fracture energy and toughness of UHPC.

Keywords: hybrid fiber, ultra-high-performance concrete, tensile behavior, fracture energy, microstructures

OPEN ACCESS

Edited by:
Kequan Yu,
Tongji University, China

Reviewed by:
Xing-yan Shang,
Shandong Jianzhu University, China
Ru Mu,
Hebei University of Technology, China

****Correspondence:***
Zongcai Deng
dengzc@bjut.edu.cn

Specialty section:
This article was submitted to Structural Materials, a section of the journal Frontiers in Materials

Received: *02 September 2021*
Accepted: *06 October 2021*
Published: *17 November 2021*

Citation:
Li J and Deng Z (2021) Tensile Behavior of Hybrid Fiber-Reinforced Ultra-High-Performance Concrete. Front. Mater. 8:769579. doi: 10.3389/fmats.2021.769579

INTRODUCTION

Ultra-high-performance concrete (UHPC) should not only have ultra-high compressive strength but also have good tensile properties, crack resistance, and toughness. The brittleness of ultra-high strength concrete increases obviously, and how to reduce its brittleness and improve its ability to resist fracture after a crack is very important (He et al., 2021). The effective way to improve the tensile properties and toughness of UHPC is usually to use high-performance fiber toughening technology (Kim et al., 2018). Steel fiber has the function of strengthening and toughening, but adding more steel fiber will increase the cost and reduce the workability of UHPC. When the crack width is small, the crack resistance and reinforcement effect of steel fiber is obvious. When the deformation is large, the steel fiber slides obviously, and the toughening effect is reduced (Deng et al., 2020), while the coarse non-metallic fibers play an obvious role in improving the deformation capacity of UHPC. Steel fibers and non-metallic fibers are mixed with complementary advantages, and give full play to the strengthening and toughening effects of fibers of different varieties and sizes, improve the fracture energy of UHPC, reduce the preparation cost, and promote the development of UHPC preparation technology and engineering application.

Kobayashi et al. (1982) first proposed the concept of hybrid fiber, that is, steel fiber and polypropylene (PE) fiber were mixed into concrete. In the later researches, most researchers studied the mechanical properties of hybrid fiber-reinforced concrete under different loading modes by changing the types and the fiber volume fraction of the hybrid fiber. The types of

hybrid fiber can be mainly divided into three categories, namely, steel–steel hybrid fiber, steel–polymer hybrid fiber, and polymer–polymer hybrid fiber (Guo et al., 2019).

In recent years, there are many reports on steel–steel hybrid fiber concrete. Park et al. (2012) investigated the effect of steel fiber on the tensile properties of ultra-high-performance hybrid fiber concrete (UHP-HFRC). The results showed that the overall shape of the tensile stress–strain curve of UHP-HFRC mainly depended on the type of macrofiber, although the addition of microfiber was conducive to strain hardening and multiple cracking behaviors. Chun et al. (2019) discussed the impact of mixed use of macro- and microsteel fibers on the pullout and tensile properties of UHPC. Kazim et al. (Turk et al., 2021) studied the effects of macro- and microsteel fiber mixing with different volume contents on the mechanical properties of self-compacting concrete. The test results showed that the hybrid-reinforced concrete specimen showed excellent ductility compared with the single macrosteel fiber-reinforced concrete specimen. Chang et al. (2020) found that the compressive strength and flexural strength of hybrid steel fiber-reinforced sulfoaluminate cement-based reactive powder concrete were effectively improved with an increase in the content of steel fibers. Steel fibers, as a kind of fiber that are seeing great attention worldwide, are widely studied by many researchers since they can improve the toughness of concrete (Kim et al., 2011; Yoo et al., 2017; Fantilli et al., 2018; Yoo et al., 2020). There are also many reports about polymer–polymer hybrid fibers (Ahmed et al., 2011; Silva et al., 2013; Pan et al., 2015; Banyhussan et al., 2016; Gong et al., 2020; Sükrü et al., 2020; Turk et al., 2021).

As we all know, steel fiber has the effect of strengthening and toughening, but adding more steel fibers will increase the production cost and reduce the workability. Recent research works reported that non-metallic fibers could also be used in UHPC instead of steel fibers (Kang et al., 2016). However, the addition of non-metallic fibers alone may reduce the workability of UHPC and expand the crack width, although it will improve the tensile ductility. Steel fiber and non-metallic fiber are mixed and complementary, to give full play to the strengthening and toughening effects of fibers of different varieties, different scales, and different stress stages. Rashiddadash et al. (2014) found that hybrid fiber-reinforced concrete with 0.75% steel fibers and 0.25% PE fibers had higher toughness indexes, modulus of rupture, and impact resistance than other hybrid mixtures. Kang et al. (2016) studied the effects of the mixed combination of 0.2-mm-diameter steel fiber and microfibers on the mechanical properties of UHPC. The test results showed that the combination of high-strength synthetic fiber (such as PE fiber) and steel fiber can improve the tensile properties of UHPC, and basalt fiber can effectively improve the tensile strength of UHPC. In the same year, Kang (Kang et al., 2016) proposed a method to improve the tensile ductility and control crack width of UHPC, and to examine the effect of artificial flaws and fiber hybridization on the tensile behavior of UHPC. Kim et al. (2019) investigated several factors affecting the efficiency of mixing steel fiber and PE fiber to improve the compressive strength and tensile properties of UHPC. The tensile strength also decreased with the increase in PE fiber content, and the strain capacity and energy absorption capacity per unit volume increased significantly after adding PE fiber. Yoo et al. (2019) considered three different types of steel fibers and four different replacement ratios of steel fibers to PE fibers, and high-energy absorbent ultra-high-performance hybrid steel and PE fiber-reinforced concrete were successfully developed at a 2% fiber volume fraction. Tran et al. (2021) examined the use of polyamide fibers in improving strain rate sensitivity and impact tensile resistance of hybrid ultra-high-performance fiber-reinforced concrete. Li et al. (2020) investigated the flexural performance of a hybrid polyethylene–steel fiber-reinforced ultra-high-performance concrete. In addition, scholars also studied multi-wall carbon nanotube (CNT) (Yoo et al., 2018), bagasse fiber (Tian et al., 2015), and polyvinyl alcohol (PVA) fiber (Yu et al., 2021). At present, different scholars have carried out a lot of research on hybrid fiber concrete, but the types of fibers need to be expanded. In addition, there are a few studies on hybrid reinforcement of UHPC with coarse and fine fibers.

In this paper, steel fibers were mixed with polyolefin (PP) fiber, PVA fiber, polyester (PET) fiber, and basalt fiber (BF). Through the direct tensile test, the contribution of hybrid fiber to the improvement of UHPC tensile properties was studied, and the tensile properties of UHPC reinforced by different varieties and sizes were compared. The test results will provide a reference for selecting fiber varieties, determining fiber geometry, and preparing high-toughness UHPC.

EXPERIMENTAL PROGRAM

Materials

The raw materials used in the test include the following: The cement is P.O. 52.5 ordinary Portland cement. The SiO_2 content of the silica fume is 95%, and the ignition loss at 950°C is 1%. The mineral powder is S95 granulated blast furnace slag powder. The diameter of quartz sand is 0.18–2 mm. Superplasticizer is added to get the appropriate workability. Mixing water is the daily water. The mix proportion of the UHPC matrix is shown in **Table 1**.

The steel fiber used to prepare UHPC was copper-plated and endless hook-shaped steel fiber and its mechanical parameters are listed in **Table 2**. To study the strengthening and toughening effect of different hybrid fiber-reinforced UHPC, different kinds of non-metallic fibers were added to the steel fiber–UHPC system: PP fiber, PVA fiber, PET fiber, and BF fiber.

All non-metal fibers were named in the form A-b-c, where A represented the fiber type, b represented the fiber length, and c represented the fiber diameter. For example, the PP-40-0.6 represented that the non-metal fiber selected for the hybrid fiber-reinforced UHPC was PP fiber, with a length of 40 mm and a diameter of 0.6 mm. The photos of non-metal fiber are shown in **Figure 1**.

TABLE 1 | Mix proportion of ultra-high-performance concrete (UHPC) matrix.

Cement	Silica fume	Mineral powder	Quartz sand	Water	Superplasticizer
556	101	354	1,213	182	11

TABLE 2 | Steel fiber properties.

Type	Length/mm	Diameter/mm	Aspect ratio	Tensile strength/MPa	Elastic modulus/GPa
CW01–0.2/13	13	0.2	65	2,850	210

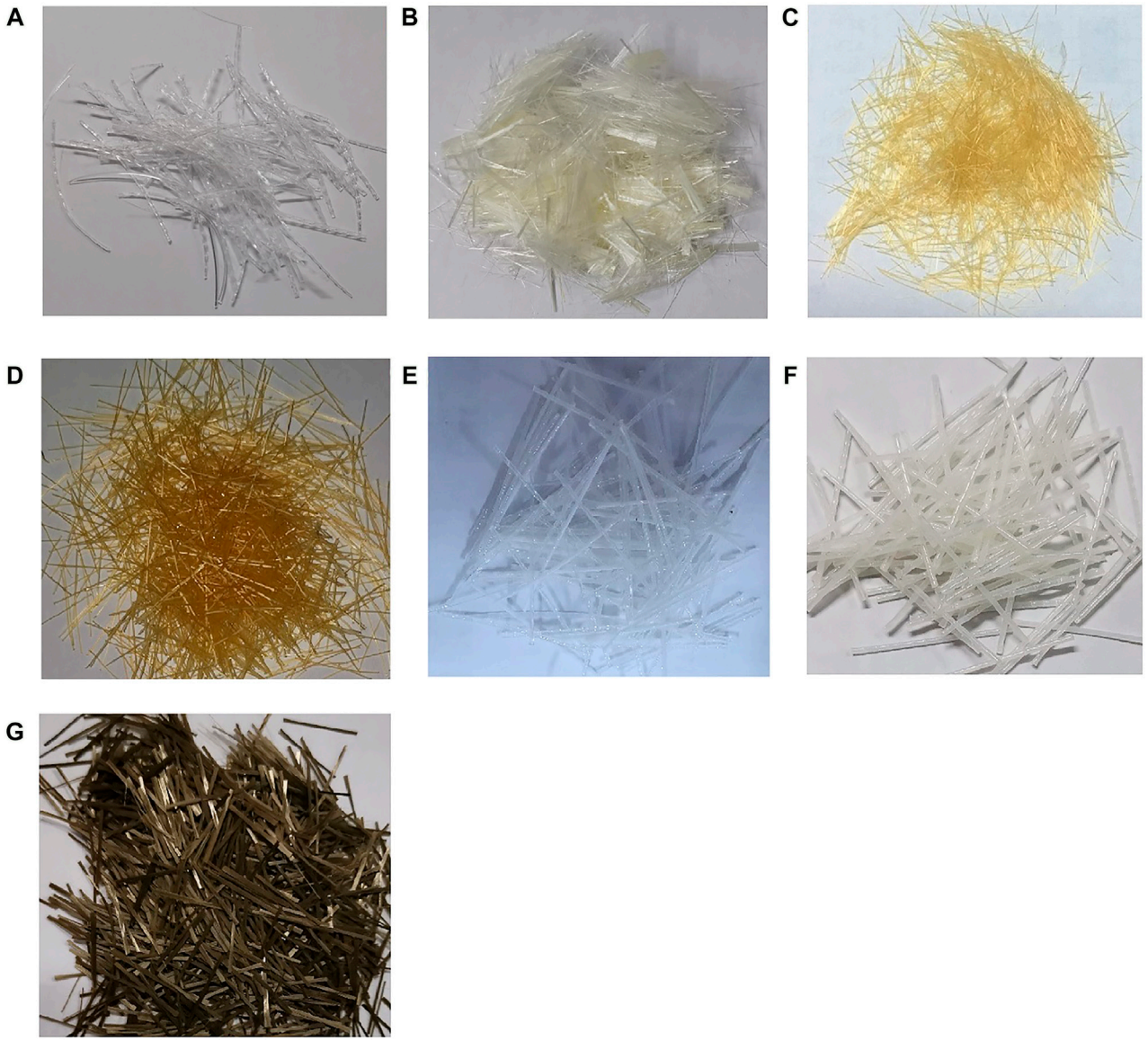

FIGURE 1 | Photos of non-metallic fibers. **(A)** PP-40-0.6, **(B)** PVA-12-0.04, **(C)** PVA-8-0.2, **(D)** PVA-12-0.2, **(E)** PET-30-0.75, **(F)** PET-30-0.9, and **(G)** BF-12-0.02.

TABLE 3 | Performance parameters of different fibers.

Type	Length/mm	Diameter/mm	Elastic modulus/GPa	Tensile strength/MPa	Density/(kg/m^3)	Fine or coarse
PP-40-0.6	40	0.6	8	650	910	Coarse
PVA-12-0.04	12	0.04	40	>1,600	1,640	Fine
PVA-8-0.2	8	0.2	35	>1,500	1,640	Coarse
PVA-12-0.2	12	0.2	39	>1,600	1,640	Coarse
PET-30-0.75	30	0.75	8	380	1,380	Coarse
PET-30-0.9	30	0.9	8	380	1,380	Coarse
BF-12-0.02	12	0.02	90	2,300	2,650	Fine

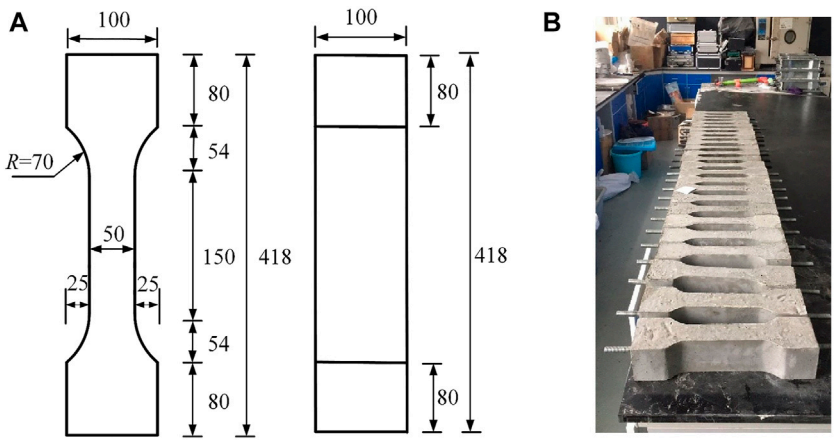

FIGURE 2 | Tensile specimens. **(A)** Dimensions of tensile specimens. **(B)** Photos of tensile specimens.

TABLE 4 | Specimen details.

Specimen ID	v_{f1}/%	Non-metallic fiber type	v_{f2}/%	Number of identical specimens
S0	0	—	—	3
S1.3	1.3	—	—	3
S1.8	1.8	—	—	3
S1.3PP0.5-40	1.3	PP-40-0.6	0.5	3
S1.3PVA0.5-12a	1.3	PVA-12-0.04	0.5	3
S1.3PVA0.5-8	1.3	PVA-8-0.2	0.5	3
S1.3PVA0.5–12 b	1.3	PVA-12-0.2	0.5	3
S1.3PET0.5-30a	1.3	PET-30-0.75	0.5	3
S1.3PET0.5-30b	1.3	PET-30-0.9	0.5	3
S1.3B0.5-12	1.3	BF-12-0.02	0.5	3

Note. v_{f1} *represented the steel fiber volume content;* v_{f2} *represented the non-metallic fiber volume content.*

The mechanical parameters of non-metallic fibers are listed in **Table 3**. Referring to the Chinese standard: technical specification for fiber-reinforced concrete structures (CECS 38:2004) (CECS 38:2004, 2004), it was considered that a fiber diameter less than 0.1 mm was fine fiber, and a fiber diameter greater than 0.1 mm was coarse fiber.

Design of Experiment

A total of 10 groups of specimens were designed, including 7 groups of hybrid fiber-reinforced UHPC specimens, 2 groups of single-doped steel fiber UHPC specimens, and 1 group of non-fiber UHPC specimens. The specimen was the dog bone shape (GB/T 50081-2019, 2019; T/CBMF 37-2018, 2018; Zhao et al., 2019; Cai et al., 2021; Yu et al., 2021), as shown in **Figure 2**, and the details of the specimens are shown in **Table 4**. The fiber volume content of all hybrid fiber-reinforced UHPC specimens was maintained at 1.8% (steel fiber:1.3%, non-metallic fiber: 0.5%), and three parallel specimens were poured for each group of specimens. When each group of specimens was casting, three UHPC cubes (100 mm × 100 mm × 100 mm)

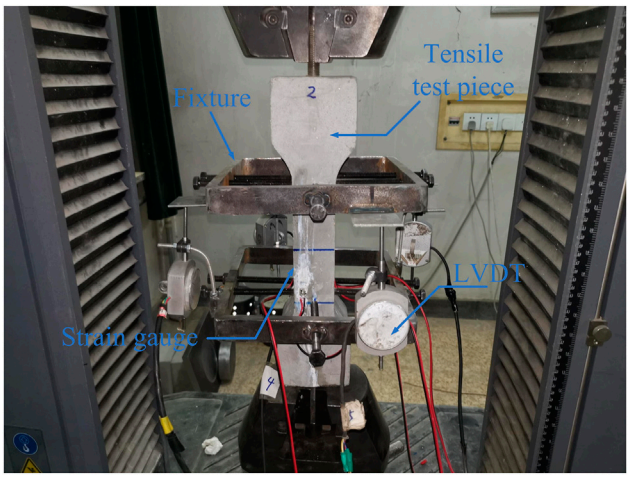

FIGURE 3 | Test setup.

were poured to obtain the compressive strength (f_{cu}). All the specimens and UHPC cubes were placed in a normal temperature environment and cured until the test.

According to the type of fiber mixed in UHPC, the hybrid fiber-reinforced UHPC specimens were named Sx-Ay-z, where S represented steel fiber, x represented steel fiber volume content; A represented the non-metallic fiber type, y represented the non-metallic fiber volume content, and z represented the non-metallic fiber length. In particular, PVA fibers with a length of 12 mm and PET fibers in this experiment had the same fiber length but different diameters. Therefore, the name of the specimen was distinguished by a and b, and a was the one with finer fiber diameter. For example, the S1.3PET0.5-30a that represented the steel fiber volume content was 1.3%, PET fiber volume content was 0.5%, the length was 30 mm, and the diameter was 0.75 mm.

The single-doped steel fiber specimen was named Sx, where S represented steel fiber, and x represented the steel fiber volume content. For example, the S1.3 that represented steel fiber volume content was 1.3%. Since three parallel specimens were poured in each group, the parallel specimens were distinguished by /1, /2, and /3. For example, the three parallel test specimens of S1.3 were named S1.3/1, S1.3/2, and S1.3/3 in turn.

Instrumentation and Test Procedure

All specimens were tested using the 300-kN MTS testing machine. To accurately measure the deformation of the specimen, a steel loading and fixing system was designed for the experiment. Four linear variable differential transducers (LVDTs) were arranged on the surface of the specimen to measure the axial deformation of the specimen over a gauge length of 150 mm. Two concrete strain gauges were arranged to assist in measuring the axial strain of the specimen. The loading was conducted by displacement control with a rate of 0.15 mm/min, and the test setup is shown in **Figure 3**.

RESULTS AND DISCUSSION

Failure Modes

Taking the specimen S1.3PET0.5-30a as an example, the typical failure mode is shown in **Figure 4**. At the initial stage of loading, the specimen did not have obvious change. With the loading continuing, the specimens would crack at the weak section of the weak position. After the specimen cracked, the UHPC at the cracked site gradually withdrew from work, the deformation continued to increase, and the cracks continued to develop around the specimen. At this time, the geometric centroid and force of the specimen were not in a straight line, eccentric tension occurred, and the UHPC on the other side may produce compressive stress at the moment. With the development of deformation, the two ends of the main crack continue to expand

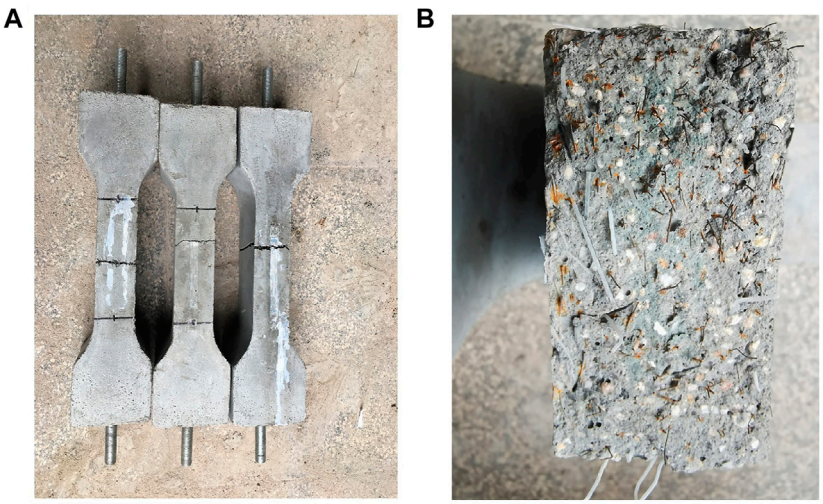

FIGURE 4 | Typical failure mode. **(A)** Failure mode of specimen. **(B)** Fracture failure state of specimens.

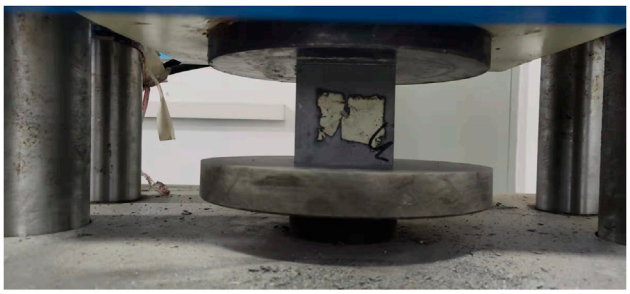

FIGURE 5 | Test setup for compressive strength.

and extend, and the specimen showed full cross-section tension until the bearing capacity was lost. After the specimen was cracked, the specimen made a "crack" sound, and the tensile stress fluctuated immediately. The sound was produced by the fibers being continuously pulled out, which reflected the bridging effect of the fibers.

It was worth noting that the failure mode of the plain UHPC specimen without fiber was different from that of the fiber-reinforced UHPC specimen. When the plain UHPC specimen was loaded to the peak tensile strength, the full section was suddenly divided into two parts, and the failure had no ductility.

The tensile properties of different hybrid fiber-reinforced UHPC were also different: the specimens mixed with PVA fiber or BF fiber with high elastic modulus and high aspect ratio (length/diameter) had a long process from loading to cracking, especially the specimens that had obvious strain-hardening characteristics before cracking, and the failure process of the specimens was slow. PP fiber and PET fiber with low elastic modulus and low aspect ratio can effectively reduce the later crack propagation rate.

Effect of Hybrid Fiber on Compressive Properties of Ultra-High-Performance Cement

All UHPC cubes (100 mm × 100 mm×100 mm) were tested for compressive strength with a 2,000-kN MTS testing machine, and the test setup is shown in **Figure 5**. The loading was conducted with stress control with a rate of 1.0 MPa/s. At the end of the test, the plain UHPC without fiber was suddenly broken at the peak load with a fragmentation, showing the characteristics of brittle failure. On the contrary, hybrid fiber-reinforced UHPC still maintained good integrity after failure, reflecting the bridging effect of fibers.

The average cube compressive strength f_{cu} of UHPC in each group is listed in **Table 5**. The compressive strength of UHPC increased by 26.1% and 32.4% when the steel fiber content increased from 0 to 1.3% and 1.8%, respectively, indicating that steel fiber had a significant reinforcing effect on UHPC. This was because steel fibers were randomly distributed in the UHPC. When the UHPC was deformed under compression, the tension of the steel fibers would indirectly increase the compressive strength of UHPC. In addition, the steel fiber also changed the failure mode of the UHPC. The plain UHPC specimen was crushed when it was damaged, while the UHPC with steel fibers still had good integrity when it was damaged, which also reflected the bridging effect of fiber.

Compared with the single-doped steel fiber specimen S1.8, the compressive strength of some hybrid fiber-reinforced UHPC specimens were reduced, and only the compressive strength of specimens S1.3PP0.5-40 and S1.3PET0.5-30b did not decrease. It showed that with the addition of non-metal fibers, the compressive strength of UHPC may be reduced. The reasons may be that the fibers of different types and sizes were dispersed in the UHPC matrix, resulting in uneven distribution of mixed fibers in the UHPC matrix and increasing some original defects.

Effect of Hybrid Fiber on Tensile Properties of Ultra-High-Performance Concrete

Tensile Stress–Strain Curve

To compare the differences of tensile properties of different types of fiber-reinforced UHPC, the typical tensile stress–strain curves of each group of specimens are shown in **Figure 6**. Due to the large ultimate deformation of hybrid fiber-reinforced UHPC, to more intuitively compare the differences in the whole failure process of different specimens, the process from loading to cracking of each group of specimens was enlarged and placed at the upper right of **Figure 6**. The tensile stress–strain curves of different hybrid fiber-reinforced UHPC can be divided into two

TABLE 5 | Average values of test results.

Specimen ID	f_{cu}/MPa	σ_p/MPa	$\varepsilon_p/\mu\varepsilon$	E_t/GPa	G_F/(N/m)	L_{ch}/mm
S1.3PP0.5-40	121.44	4.27	121	36.89	13,724.29	27,767.88
S1.3PVA0.5-12a	101.15	5.13	254	42.32	28,054.24	45,112.80
S1.3PVA0.5-8	108.14	4.74	192	37.23	31,447.36	52,109.94
S1.3PVA0.5-12 b	106.15	4.95	116	55.83	22,206.54	50,598.56
S1.3PET0.5-30a	108.30	5.07	139	44.50	23,771.44	41,152.82
S1.3PET0.5-30 b	119.79	4.18	85	40.21	12,638.43	29,085.37
S1.3B0.5-12	107.26	5.44	189	45.12	16,586.55	25,288.75
S0	91.51	4.16	101	36.91	—	—
S1.3	115.35	4.73	109	38.60	10,954.26	18,899.4
S1.8	121.13	5.21	110	40.53	32,602.58	48,680.29

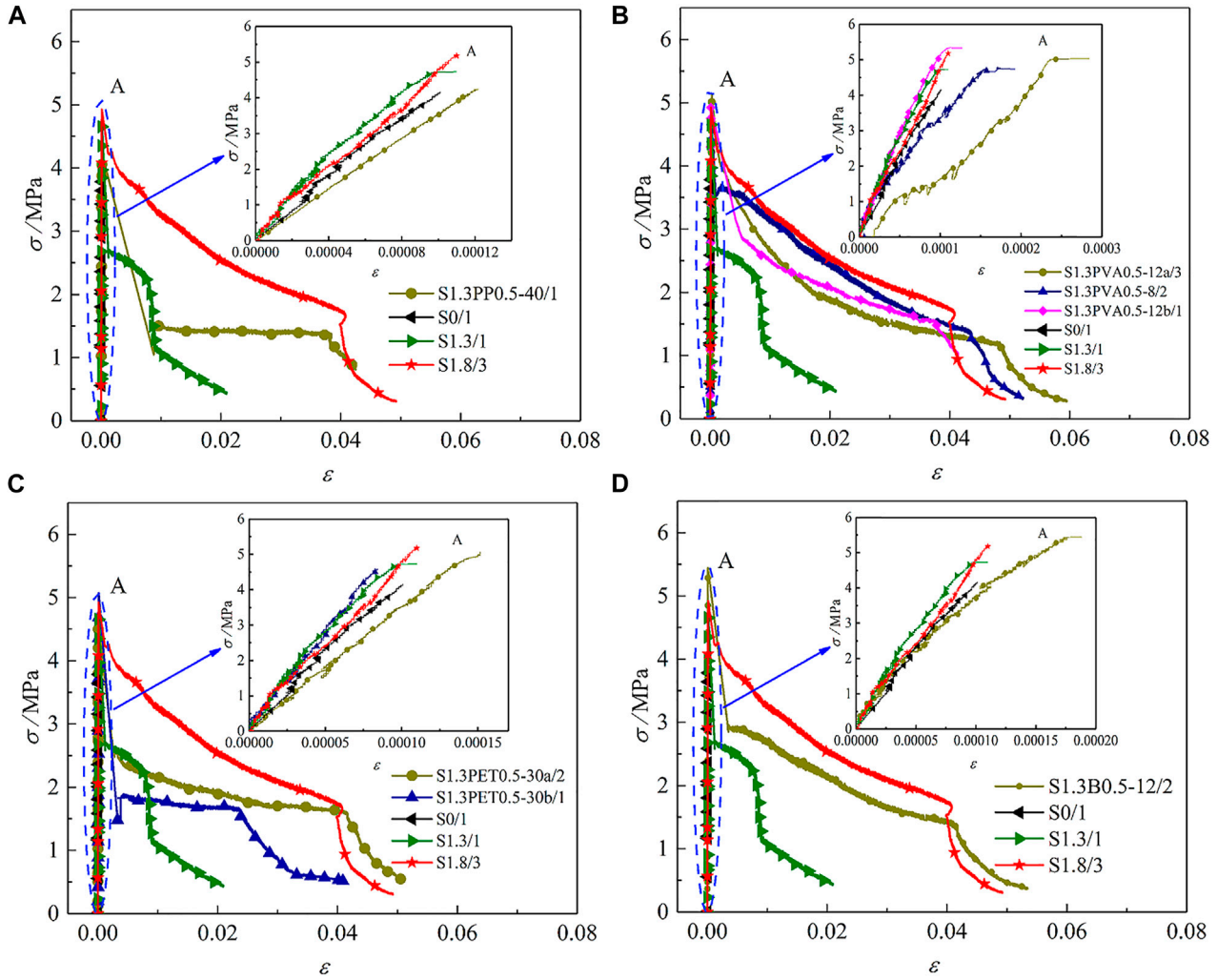

FIGURE 6 | Tensile stress–strain curve. **(A)** S1.3PP0.5. **(B)** S1.3PVA0.5. **(C)** S1.3PET0.5. **(D)** S1.3B0.5.

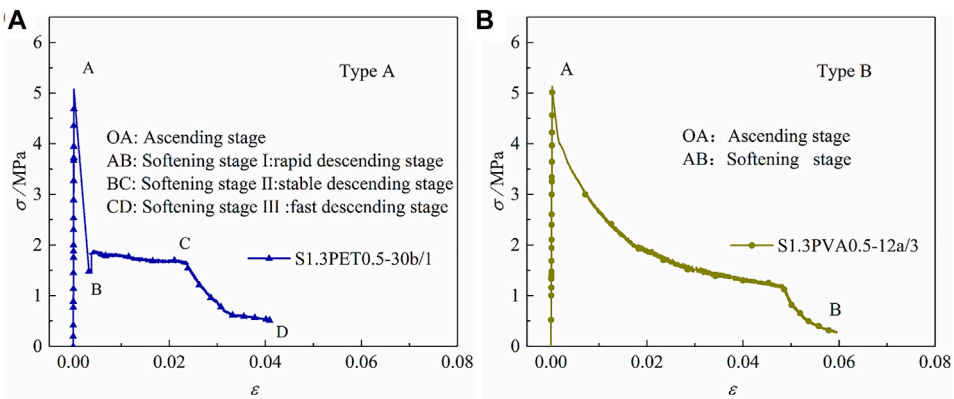

FIGURE 7 | Two types of strain-softening ultra-high-performance concrete (UHPC) tensile complete curves. **(A)** Type A. **(B)** Type B.

parts: ascending and softening branches. Due to the different types and volume content of fibers, the tensile stress–strain curves can be divided into two different types (Type A and Type B). The ascending branches of the tensile curve of the two types of strain-softening UHPC were similar, and the softening branches were different, as shown in **Figure 7**.

Type A: generally, the tensile stress–strain curve of UHPC with low fiber content or hybrid steel fiber and long or coarse non-metallic fiber. It can be divided into four stages: 1) Ascending stage: The relationship between stress and strain is approximately linear until microcracks appear in the specimen. At this stage, the single-doped steel fiber or hybrid fiber effectively reduces the possibility of stress concentration in the matrix. When the tensile stress increases to the initial crack stress, microcracks appear in the component, the cracked UHPC loses its bearing capacity, and the fibers crossing the cracks begin to play a role. Generally, some microfibers have low elastic modulus but have a large number, which can significantly inhibit the development of early microcracks. Compared with ordinary concrete, the generation and expansion of initial cracks of fiber concrete are delayed; 2) Softening stage I: rapid descending stage. After the specimen reaches the tensile strength, it cracks, and the bearing capacity decreases rapidly. This kind of curve often shows that the fiber content is low, or the steel fiber is mixed with long or coarse non-metallic fibers, and these fibers begin to play a bridging role gradually after the specimen cracks. Therefore, the bearing capacity of the specimen decreases suddenly at the moment of cracking. This stage is closely related to the type and content of fiber in the specimen. When the fiber content or type is appropriate, the bearing capacity of the specimen decreases only slightly. On the contrary, the bearing capacity of the specimen will decrease greatly; 3) Softening stage II: stable descending stage. At this stage, with the increase in crack width, the fibers between cracks, especially some macrofibers, begin to play a bridging role. The fiber is well bonded with the matrix, which can effectively delay and prevent the expansion of cracks, improve the toughness of the matrix, and maintain the stability of bearing capacity; 4) Softening stage III: fast descending stage. As the fibers are continuously pulled out or broken, the fiber-bridging effect is gradually weakened, and the bearing capacity of the specimen decreases rapidly with the increase in specimen deformation.

Type B: generally, the UHPC tensile stress–strain curve with high fiber content or hybrid steel fiber and fine non-metallic fiber. It can be roughly divided into two stages: 1) Ascending stage, which is similar to the ascending section of type A. Since microfibers can inhibit the development of early microcracks, strain hardening is more likely to occur before specimen cracking than type A. 2) Softening stage: After the specimen is cracked, the fibers between the cracks effectively play a bridging role to control the extension of macrocracks, and the bearing capacity does not decrease rapidly. Compared with the tensile stress–strain curve of type A, the softening section is gentler and shows good toughness.

It can be seen from the tensile stress–strain curve of the hybrid PP fiber in **Figure 6A** that the coarse PP fiber had little effect on the ascending stage, but the tensile peak strain was slightly increased. After the specimen S1.3PP0.5-40 cracked, the tensile stress dropped significantly. The reason was that the diameter of the PP fiber was too coarse, and the effect of controlling the expansion of microcracks before cracking was not obvious. When the specimen was cracked, the PP fibers between the cracks cannot immediately play a bridging role, so the stress decreased. Compared with the single-doped steel fiber specimen S1.3, the descending stage of the specimen S1.3PP0.5-40 was gentler, and the toughening effect was obvious.

It can be seen from the tensile stress–strain curve of hybrid PVA fiber in **Figure 6B** that before cracking, the specimens S1.3PVA0.5-12a, S1.3PVA0.5-8, and S1.3PVA0.5-12b had obvious strain-hardening characteristics, reflecting the good crack resistance of PVA fiber. Among them, fiber PVA-12-0.04 had the best crack resistance, followed by PVA-8-0.2, and PVA-12-0.2 was inferior. The reason was that the diameter of the three PVA fibers was relatively small, and the elastic modulus was medium. Before cracking, they can effectively delay the development of microcracks, improve the crack resistance of the specimen, and improve the tensile strength of the specimen, which had an obvious effect of strengthening the crack resistance. Compared with specimen S1.3, the descending section of the specimens S1.3PVA0.5-12a, S1.3PVA0.5-8, and S1.3PVA0.5-12b was gentle, and the ultimate deformation was large. The reason was that there were hydroxyl groups on the surface of the PVA fiber, which was well bonded with the UHPC matrix and which can effectively control the development of macrocracks, reflecting the good toughening effect of the PVA fiber.

It can be seen from the tensile stress–strain curve of hybrid PET fiber in **Figure 6C** that before cracking, specimen S1.3PET0.5-30a had strain-hardening characteristics, while specimen S1.3PET0.5-30b had no strain hardening characteristics. After cracking, the descending section of S1.3PET0.5-30a was gentle, and the ultimate strain was large, which reflected the good crack resistance and toughening effect of fiber PET-30-0.75. The tensile stress of specimen S1.3PET0.5-30b decreased greatly after cracking, and the descending section was also relatively gentle, which also reflected the crack resistance and toughening effect of the fiber PET-30-0.9. A comprehensive comparison found that the crack resistance and toughening effect of the fiber PET-30-0.9 were weaker than that of the fiber PET-30-0.75. The reason was that the diameter of the fiber PET-30-0.9 was too thick, and the number of fibers per unit cross-sectional area was too small. Therefore, it was suggested that the diameter of fiber PET should not exceed 0.75 mm.

It can be seen from the tensile stress–strain curve of hybrid BF fiber in **Figure 6D** that before cracking, the specimen S1.3B0.5-12 had obvious strain-hardening characteristics, and the tensile strength had been significantly improved. At the moment of cracking, the bearing capacity decreased obviously, and then the descending section was gentle. It can be seen that the BF fiber had a fine diameter and high elastic modulus, which has an obvious strengthening and toughening effect.

To better quantitatively compare the differences in tensile properties of each group of specimens, the strength corresponding to the peak point was taken as the tensile strength (σ_p), and its corresponding strain was taken as the

peak strain (ε_p). Take the slope of the connecting line between 5% and 50% of the maximum stress in the ascending stage of the tensile stress–strain curve of the specimen as the elastic modulus (E_t). To evaluate the performance differences of the different specimens after cracking, fracture energy (G_F) was defined to characterize the energy absorption capacity of the specimens and characteristic length (L_{ch}) to characterize the brittleness of the specimens. All the above results were the average values of the same group of parallel specimens, and the results are listed in **Table 5**.

Effect of Hybrid Fiber on Tensile Strength

The tensile strength σ_p of UHPC in each group is listed in **Table 5**. When the steel fiber content increased from 0 to 1.3% and 1.8%, the tensile strength of UHPC increased by 13.70% and 25.24% respectively, indicating that the tensile strength of UHPC can be significantly improved by adding steel fibers. In addition, the addition of steel fibers also changed the brittle failure characteristics of the plain UHPC. After the peak tensile strength, the descending section of specimen S1.8 was gentler than that of S1.3. This was because the steel fibers played a great role before and during the cracking of UHPC. The steel fiber exerted its bridging function and continuously transmitted the stress to the surrounding matrix so that the matrix can continue to work under the stress after it was cracked, which cannot only increase the tensile stress but also improve the ability to resist tensile deformation.

Compared with S1.3, the tensile strength of S1.3PP0.5-40 and S1.3PET0.5-30b decreased by 9.73% and 11.63%, respectively, and the tensile strength of S1.3PVA0.5-12a, S1.3PVA0.5-8, S1.3PVA0.5-12b, S1.3PET0.5-30a, and S1.3B0.5-12 increased by 8.46%, 0.03%, 4.65%, 7.19%, and 15.01%, respectively. Generally speaking, microfibers can effectively prevent the development of microcracks, and macrofibers can effectively prevent the development of cracks after macrocracks appeared (Fantilli et al., 2017; Stahli and Mier 2007). Therefore, some fine fibers such as PVA-12-0.04 and BF-12-0.02 had an obvious enhancement effect on the matrix. Some coarse fibers such as PP-40-0.6 and PET-30-0.9 cannot prevent the development of microcracks well before the specimen cracked, so the tensile strength of the specimen was significantly reduced.

The tensile strength of the specimen hybrid with three different sizes of PVA fiber and steel fiber was improved. The reinforcement effect of the two PVA fibers with a length of 12 mm was better than that of the PVA fiber with a length of 8 mm. The length of fiber PVA-12-0.04 and PVA-12-0.2 was the same as 12 mm, but the diameter of fiber PVA-12-0.04 was only 0.04 mm, so its reinforcement effect was the best.

Among all the hybrid fiber-reinforced UHPC specimens, the tensile strength of specimen S1.3B0.5-12 was the highest, even higher than that of specimen S1.8, indicating that the reinforcement effect of fiber BF-12-0.02 was the best among all non-metallic fibers because its minimum diameter was only 0.02 mm, and its elastic modulus was the highest among all non-metallic fibers. Therefore, selecting fine fibers with high elastic modulus was the most effective way to improve the tensile strength of materials.

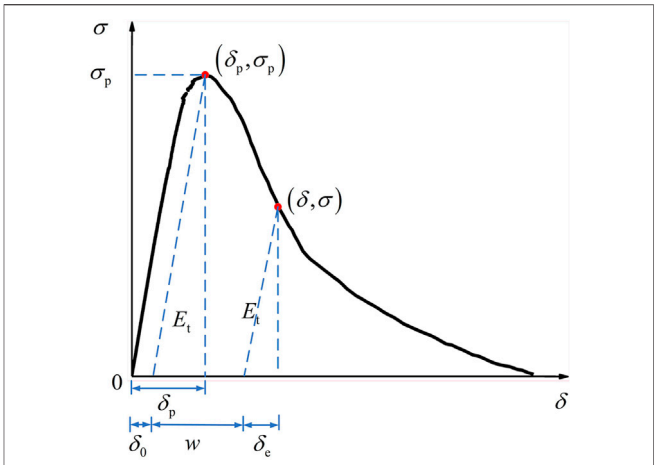

FIGURE 8 | Schematic diagram of UHPC tensile stress–total deformation curve.

Effect of Hybrid Fiber on Peak Strain

The peak strain ε_p of UHPC in each group is listed in **Table 5**. When the steel fiber content increased from 0 to 1.3% and 1.8%, the peak strain of UHPC was close.

Compared with S1.8, the peak strain of S1.3PET0.5-30b decreased by 22.73%, and the peak strain of S1.3PP0.5-40, S1.3PVA0.5-12a, S1.3PVA0.5-8, S1.3PVA0.5-12b, S1.3PET0.5-30a, and S1.3B0.5-12 increased by 10.00%, 110.00%, 74.55%, 5.45%, 26.36%, and 71.81%, respectively. Similar to the effect of hybrid fibers on tensile strength, in general, microfibers can effectively prevent the development of microcracks, and macrofibers can effectively prevent the development of cracks after macrocracks appeared (Fantilli et al., 2017; Stahli and Mier 2007).

For three different sizes of PVA fiber and steel fiber hybrid-reinforced UHPC specimens, the peak strain of specimens S1.3PVA0.5-12a, S1.3PVA0.5-8, and S1.3PVA0.5-12b decreased in turn. The reason was that the diameter of fiber PVA-12-0.04 was only 0.04 mm, and the number of fibers contained in the unit cross-sectional area was the largest, which also reflected the contribution of micro-fibers to slowing down the initiation and development of microcracks.

Compared with S1.3PET0.5-30a, the peak strain of S1.3PET0.5-30b decreased by 38.85%. The same reason was that the diameter of fiber PET-30-0.9 was too coarse, and the number of fibers contained in the section of the same area reduced, resulting in a decrease in peak strain.

In all fiber hybrid-reinforced UHPC tensile specimens, PVA-12-0.04, PVA-8-0.2, and BF-12-0.02 had a significant increase in peak strain because these three fibers had fine diameter, high elastic modulus, and excellent enhancement effect.

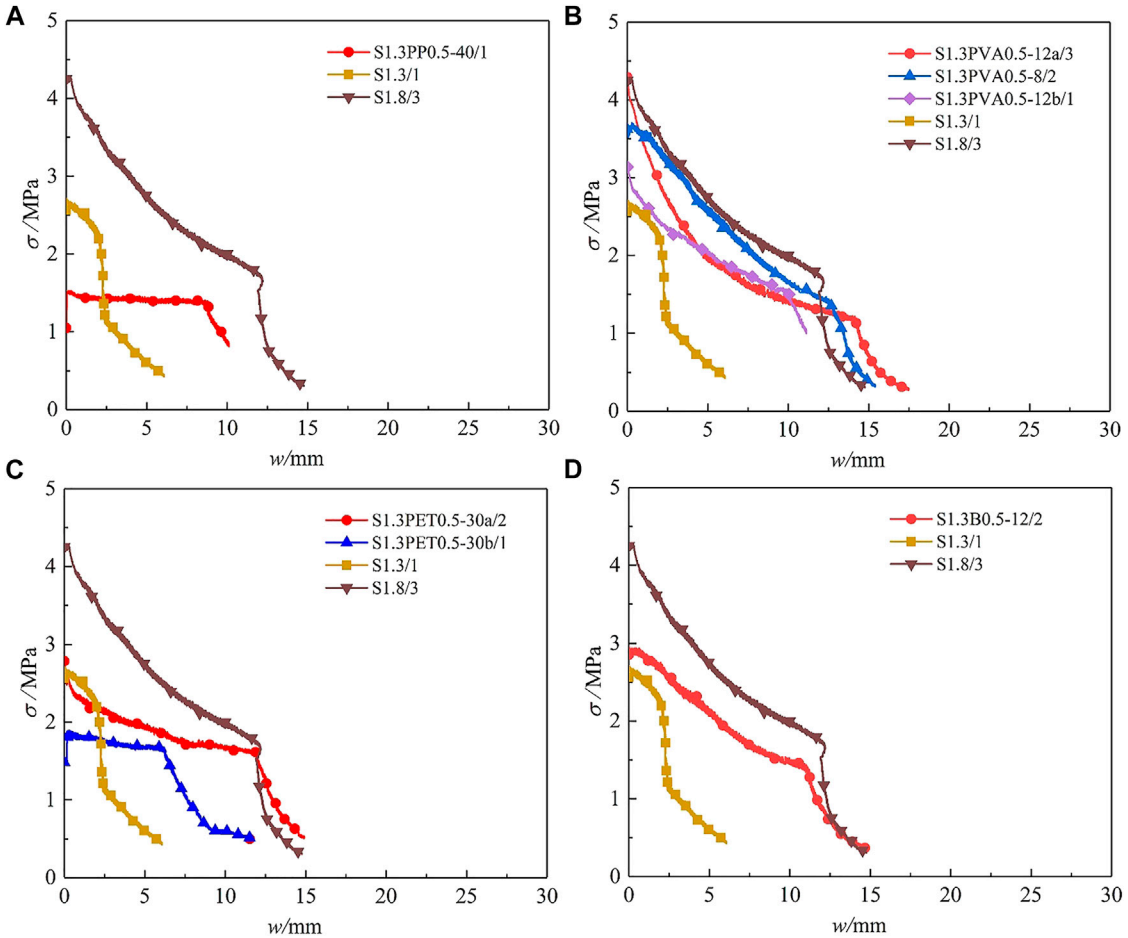

FIGURE 9 | Tensile stress-crack width curve. **(A)** S1.3PP0.5. **(B)** S1.3PVA0.5. **(C)** S1.3PET0.5. **(D)** S1.3B0.5.

Tensile Stress-Crack Width Curve

Based on the assumption that the specimen does not crack before peak load, and the residual deformation does not increase after the peak load, the schematic diagram of UHPC tensile stress–total deformation curve is shown in **Figure 8**, and the total deformation δ (Deng et al., 2009) of hybrid fiber-reinforced UHPC in the tensile process is:

$$\delta = \delta_e + \delta_0 + w \tag{1}$$

where w is the macrocrack width, and δ_e and δ_0 are the elastic deformation and residual deformation outside the fracture zone of the specimen, respectively, and then:

$$\delta_e = \frac{\sigma l}{E_t} \tag{2}$$

$$\delta_e^0 = \frac{\sigma_p l}{E_t} \tag{3}$$

$$\delta_0 = \delta_p - \delta_e^0 \tag{4}$$

where σ and σ_p are the axial tensile stress and the peak stress, respectively, δ_p and δ_e^0 are the total deformation and elastic deformation corresponding to peak stress, respectively, E_t is the elastic modulus, and l is the gauge distance of the specimen.

The crack propagation width w is independent of the length of the specimen, and there is no macrocrack before the maximum load (Deng et al., 2009). According to **Eq. 1**, the w is:

$$w = \delta - \delta_e - \delta_0 \tag{5}$$

The tensile stress–crack width curves are shown in **Figure 9**. Different hybrid fiber-reinforced UHPC had significant differences due to the different characteristics of non-metal fibers. To better evaluate the difference in tensile stress–crack width curves of different tensile specimens, the evaluation index of fracture energy (G_F) was introduced (see the *Effect of hybrid fibers on fracture energy* section for details).

Effect of Hybrid Fibers on Fracture Energy

Fracture energy G_F (Deng et al., 2009) is the energy consumed to form cracks per unit area, that is, the ratio of the area under the tensile stress–crack width curves to the cross-sectional area of the specimen, and

$$G_F = \int_0^{w_f} \sigma(w)\mathrm{d}w \quad (6)$$

The fiber-reinforced UHPC had large deformation. To compare the toughness differences of different specimens more accurately, it was uniformly taken that the load was reduced to 20% of the cracking load. The calculation results of the fracture energy of the different specimens are listed in **Table 5**. The fracture energy value reflected the energy consumed by UHPC during the fracture process. The greater the fracture energy, the greater the energy consumed by UHPC during the fracture process, and the more significant the crack resistance effect of the fiber.

Plain UHPC specimen S0 had a brittle fracture, and the fracture energy was not considered. The fracture energy of UHPC increased by 197.62% when the content of steel fiber was increased from 1.3% to 1.8%, indicating that steel fiber had a significant toughening effect on UHPC.

Compared with the single-doped steel fiber specimen S1.3, the fracture energies of S1.3PP0.5-40, S1.3PVA0.5-12a, S1.3PVA0.5-8, S1.3PVA0.5-12b, S1.3PET0.5-30a, S1.3PET0.5-30b, and S1.3B0.5-12 increased by 25.29%, 156.10%, 187.07%, 102.72%, 117.01%, 15.37%, and 53.88%, respectively. The steel fiber content of all hybrid fiber-reinforced UHPC was 1.3%, and the fracture energy was significantly improved by adding non-metallic fiber of fiber content 0.5%, which showed that the steel fiber and non-metallic fiber were mixed with complementary advantages and gave full play to the strengthening and toughening effects of fibers of different varieties and sizes. In general, long fibers can more effectively limit the development of macrocracks than short fibers, to improve the ductility of UHPC and achieve the effect of toughening. In the test, the fibers PVA-12-0.04, PVA-8-0.2, PVA-12-0.2, PET-30-0.75, and BF-0.02 all showed good toughening effects.

The fracture energy of the specimens S1.3PVA0.5-8, S1.3PVA0.5-12a, and S1.3PVA0.5-12b decreased sequentially in three different sizes of PVA fiber and steel fiber hybrid-reinforced UHPC specimens, which showed that among the three types of PVA fibers, fiber PVA-8-0.2 had the best toughening effect, followed by PVA-12-0.04, and PVA-12-0.2 was the worst.

Compared with the specimen S1.3PET0.5-30a, the fracture energy of S1.3PET0.5-30b was reduced by 47.99%. The reasons were also that the diameter of fiber PET-30-0.9 was too thick, the number of fibers contained in the section of the same area was reduced, and the bonding force between the fiber and the matrix was reduced, resulting in the decrease in fracture energy.

Compared with other non-metallic fibers, the fracture energy of all steel fiber–PVA hybrid fiber-reinforced UHPC was very high, indicating that PVA fiber had a good toughening effect due to its relatively high elastic modulus, tensile strength, and excellent dispersion. In addition, the fracture energy of the specimen S1.3PET0.5-30a was also higher, which reflected the good toughening effect of the fiber PET-30-0.75.

The fracture energy of all hybrid fiber-reinforced UHPC was lower than that of specimen S1.8, indicating that steel fiber played an important role in strengthening and toughening in the whole process of specimen tension. However, high steel fiber content would increase the cost and reduce the workability. When the crack width of steel fiber was small, the crack resistance and reinforcement effect were obvious. When the deformation was large, the steel fiber would slip obviously, and the toughening effect was reduced. Through the above test results, it can be found that the hybrid of steel fiber and non-metallic fiber can complement the advantages of each other, give full play to the strengthening and toughening effect of different varieties and different sizes of fibers, not only improve the fracture energy and toughness of UHPC but also reduce the preparation cost, and promote the development of UHPC preparation technology and engineering application.

Characteristic Length

The characteristic length L_{ch} (Deng et al., 2009) proposed by Hillerborg is usually used to express the brittle fracture performance of concrete, and

$$L_{ch} = \frac{E_t G_F}{(f_t)^2} \quad (7)$$

where the units of L_{ch} and E_t are mm and GPa, respectively, and the units of G_F and f_t are N/m and MPa, respectively. The smaller the L_{ch}, the more brittle the material.

The calculation results of the characteristic lengths of different specimens are listed in **Table 5**. The plain UHPC specimen S0 had a brittle fracture, and the characteristic length was not considered. In the specimens with single steel fiber, when the content of steel fiber increased from 1.3% to 1.8%, the characteristic length of UHPC increased by 222.73%, which showed that steel fiber had a significant toughening effect on UHPC and reduced the brittleness of the material.

Compared with the specimen S1.3, the characteristic lengths of the specimens S1.3PP0.5-40, S1.3PVA0.5-12a, S1.3PVA0.5-8, S1.3PVA0.5-12b, S1.3PET0.5-30a, S1.3PET0.5-30b, and S1.3B0.5-12 were increased by 64.83%, 167.80%, 209.33%, 200.36%, 17.36%, 259.39%, and 50.12%, respectively. The average characteristic length of ordinary mortar was 110 mm, the average characteristic length of ordinary concrete and polypropylene fiber concrete were 600 and 650 mm, respectively, the characteristic length of engineered cementitious composite (ECC) was between 1,405 and 3,461 mm (Deng et al., 2009), and the characteristic length of hybrid fiber-reinforced UHPC was between 19,700.21 and 60,542.86 mm, which reflected the good toughness of hybrid fiber-reinforced UHPC. The reason was that hybrid fiber had good crack control ability, delayed the development of cracks, and prevented the extension of macrocracks.

Superficial Microstructure Characteristics of Different Fibers

The observation results of the microstructure morphology of UHPC by scanning electron microscope (SEM) is shown in

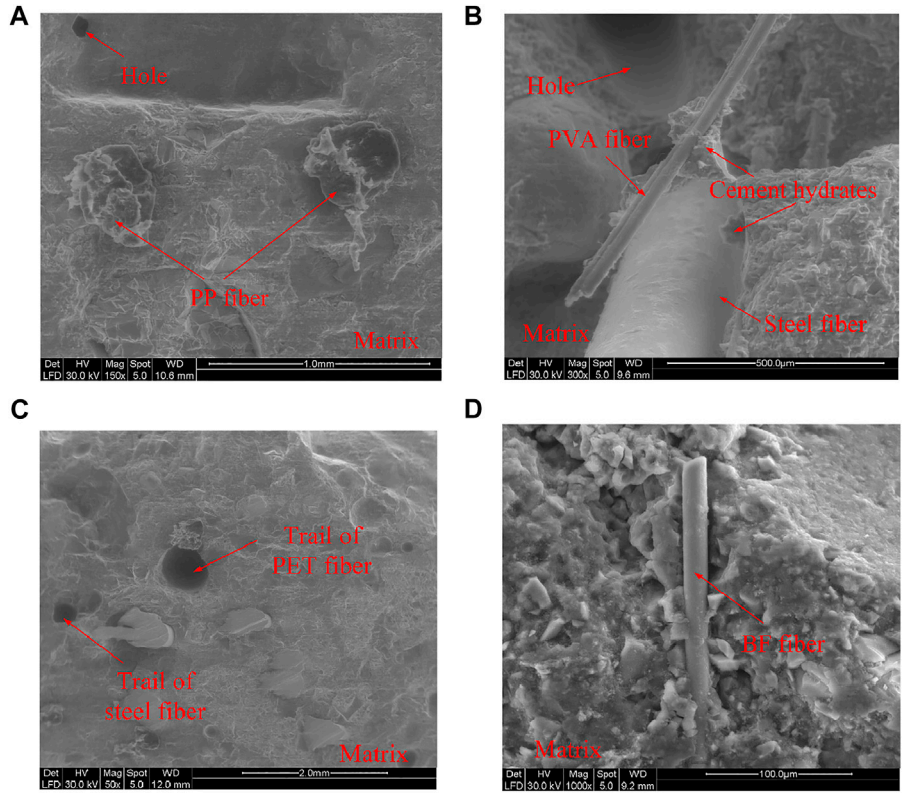

FIGURE 10 | (SEM) observations of matrix and different fiber interfaces in UHPC. **(A)** PP fiber. **(B)** PVA fiber. **(C)** PET fiber. **(D)** BF fiber.

Figure 10. Due to the low water/binder ratio, the hardened UHPC matrix was quite dense. In **Figure 10A**, the PP fibers were fully bonded with the matrix, giving full play to the bridging effect in the failure process, and delaying the expansion of local macrocracks. In **Figure 10B**, the steel fiber had a smooth surface and a small number of hydration products on the surface, which meant that the interfacial bonding strength between the matrix and the steel fiber was weak. The weaker bond strength and the higher tensile strength of steel fibers made it easier for steel fibers to pull out rather than rupture. PVA fiber had good hydrophilicity, and a large number of hydration products can be observed on the surface of the PVA fiber. These hydration products ensured better adhesion between PVA fiber and the UHPC matrix. In the early stage of failure, the PVA microfiber can effectively play the bridging role and delay the further development of microcracks. With the increase inf specimen deformation, microcracks became macrocracks. Because of its thicker diameter and longer length, steel fiber can effectively prevent the propagation of macrocracks and improve the ductility of materials until most of the steel fibers were pulled out. In **Figure 10C**, because of its large size, the PET fiber was similar to the PP fiber, mainly bridging macrocracks, and finally, most PET fibers were pulled out or ruptured. In **Figure 10D**, BF fibers were well wrapped by the UHPC matrix, which showed that BF fiber and UHPC matrix had a strong mechanical bite effect, closely bonded, and give full play to the bridging effect. In addition, BF fiber had the most obvious reinforcing effect because of its fine diameter and high elastic modulus.

CONCLUSION

In this paper, 10 groups of tensile specimens were designed, including 7 groups of hybrid fiber-reinforced UHPC specimens, 2 groups of single-doped steel fiber UHPC specimens, and 1 group of plain UHPC specimens. Seven kinds of non-metallic fiber and steel fiber were selected to carry out experimental research and theoretical analysis on different kinds, different diameters, and different lengths of non-metallic fiber–steel fiber hybrid-reinforced UHPC. The main conclusions are as follows:

1) The addition of different non-metallic fibers would reduce the compressive strength of UHPC. The reason may be that fibers of different types and sizes were dispersed unevenly in the UHPC matrix, adding to some of the original defects.
2) Hybrid fiber-reinforced UHPC tensile specimens can still bear the load after cracking, showing good ductile failure characteristics, reflecting the good crack resistance and toughening effect of different fibers.
3) The tensile stress–strain curves of UHPC with different hybrid fibers can be divided into two parts: ascending

section and softening section. Among them, the softening section was greatly affected by the type and content of fiber.

4) Some microfibers such as PVA-12-0.04 and BF-12-0.02 had an obvious reinforcing effect on the UHPC matrix, the tensile strength and peak strain of the specimen were improved. Fiber BF-12-0.02 had a fine diameter and high elastic modulus, and the reinforcement effect was the most significant.
5) Compared with the single-doped steel fiber specimen S1.3, the fibers PVA-12-0.04, PVA-8-0.2, PVA-12-0.2, PET-30-0.75, and BF-12-0.02 were added respectively, the fracture energy of the specimen was increased by 53.88%–187.07%, which reflected its good toughening effect. Among the three PVA fibers of different sizes, the fiber PVA-8-0.2 had the best toughening effect; the diameter of the coarse PET fiber should not be greater than 0.75 mm; too coarse a diameter can reduce the bonding force between fiber and matrix reducing the fracture energy.
6) The hybrid of steel fiber and non-metallic fiber can complement the advantages of each other, give full play to the strengthening and toughening effects of different varieties and sizes of fibers, not only improve the fracture energy and toughness of UHPC but also reduce the preparation cost, and promote the development of UHPC preparation technology and engineering application.

DATA AVAILABILITY STATEMENT

The original contributions presented in the study are included in the article/Supplementary Material. Further inquiries can be directed to the corresponding author.

AUTHOR CONTRIBUTIONS

JL conceptualized the study, formulated the methodology, performed the software and formal analysis, conducted data curation, and wrote and prepared the original draft. ZD reviewed and edited the manuscript, supervised the study, was in charge of the project administration, and acquired the funding. All authors have read and agreed to the published version of the manuscript.

FUNDING

This research was performed under a grant from the Beijing Municipal Education Committee funding project (Grant No. KZ201810005008).

ACKNOWLEDGMENTS

The authors would like to thank the Beijing Municipal Education Committee funding project (No. KZ201810005008) for supporting the present work.

REFERENCES

Ahmed, S. F. U., and Mihashi, H. (2011). Strain Hardening Behavior of Lightweight Hybrid Polyvinyl Alcohol (PVA) Fiber Reinforced Cement Composites. *Mater. Struct.* 44, 1179–1191. doi:10.1617/s11527-010-9691-8

Banyhussan, Q. S., Yıldırım, G., Bayraktar, E., Demirhan, S., and Şahmaran, M. (2016). Deflection-hardening Hybrid Fiber Reinforced concrete: the Effect of Aggregate Content. *Construction Building Mater.* 125, 41–52. doi:10.1016/j.conbuildmat.2016.08.020

Cai, Z., Liu, F., Yu , J., Yu, K., and Tian, L. (2021). Development of ultra-high ductility engineered cementitious composites as a novel and resilient fireproof coating. Construction Building Mater 288, 123090. doi:10.1016/j.conbuildmat.2021.123090

Chang, J., Cui, K., and Zhang, Y. (2020). Effect of Hybrid Steel Fibers on the Mechanical Performances and Microstructure of Sulphoaluminate Cement-Based Reactive Powder concrete. *Construction Building Mater.* 261, 120502. doi:10.1016/j.conbuildmat.2020.120502

Chun, B., and Yoo, D.-Y. (2019). Hybrid Effect of Macro and Micro Steel Fibers on the Pullout and Tensile Behaviors of Ultra-high-performance concrete. *Composites B: Eng.* 162, 344–360. doi:10.1016/j.compositesb.2018.11.026

Deng, F., Xu, L., Chi, Y., Wu, F., and Chen, Q. (2020). Effect of Steel-Polypropylene Hybrid Fiber and Coarse Aggregate Inclusion on the Stress-Strain Behavior of Ultra-high Performance concrete under Uniaxial Compression. *Compos. Structures* 252, 112685. doi:10.1016/j.compstruct.2020.112685

Deng, Z., Xue, H., Li, P., and Zhang, P. (2009). Uniaxial Tensile Mechanical Properties of High Ductile Fiber Reinforced Cementitious Composites. *J. Beijing Univ. Tech.* 35 (9), 1204–1208. (In Chinese).

Fantilli, A. P., Kwon, S., Mihashi, H., and Nishiwaki, T. (2018). Synergy Assessment in Hybrid Ultra-high Performance Fiber-Reinforced concrete (UHP-FRC). *Cement and Concrete Composites* 86, 19–29. doi:10.1016/j.cemconcomp.2017.10.012

Gong, T., Curosu, I., Liebold, F., Vo, D. M. P., Zierold, K., Maas, H.-G., et al. (2020). Tensile Behavior of High-Strength, Strain-Hardening Cement-Based Composites (HS-SHCC) Reinforced with Continuous Textile Made of Ultra-high-molecular-weight Polyethylene. *Materials*. 13, 5628. doi:10.3390/ma13245628

Guo, H., Tao, J., Chen, Y., Li, D., Jia, B., and Zhai, Y. (2019). Effect of Steel and Polypropylene Fibers on the Quasi-Static and Dynamic Splitting Tensile Properties of High-Strength concrete. *Construction Building Mater.* 224, 504–514. doi:10.1016/j.conbuildmat.2019.07.096

He, J., Chen, W., Zhang, B., Yu, J., and Liu, H. (2021). The Mechanical Properties and Damage Evolution of UHPC Reinforced with Glass Fibers and High-Performance Polypropylene Fibers. *Materials* 14, 2455. doi:10.3390/ma14092455

Kang, S., Choi, J., Koh, K., Lee, K., and Lee, B. (2016). Hybrid Effects of Steel Fiber and Microfiber on the Tensile Behavior of Ultra-high Performance concrete. *Compos. Struct.* 145, 37–42. doi:10.1016/j.compstruct.2016.02.075

Kang, S., Lee, K., Choi, J., Lee, Y., Felekoglu, B., and Lee, B. (2016). Control of Tensile Behavior of Ultra-high Performance concrete through Artificial Flaws and Fiber Hybridization. *Int. J. Concr. Struct. Mater.* 10 (3), 33–41. doi:10.1007/s40069-016-0155-6

Kim, D. J., Park, S. H., Ryu, G. S., and Koh, K. T. (2011). Comparative Flexural Behavior of Hybrid Ultra High Performance Fiber Reinforced concrete with Different Macro Fibers. *Construction Building Mater.* 25, 4144–4155. doi:10.1016/j.conbuildmat.2011.04.051

Kim, M.-J., Kim, S., and Yoo, D.-Y. (2018). Hybrid Effect of Twisted Steel and Polyethylene Fibers on the Tensile Performance of Ultra-high-performance Cementitious Composites. *Polymers* 10, 879. doi:10.3390/polym10080879

Kim, M., Yoo, D., and Yoon, Y. (2019). Effects of Geometry and Hybrid Ratio of Steel and Polyethylene Fibers on the Mechanical Performance of Ultra-high-

performance Fiber-Reinforced Cementitious Composites. *J. Mater. Res. Technol.* 8 (2), 1835–1848. doi:10.1016/j.jmrt.2019.01.001

Kobayashi, K., and Cho, R. (1982). Flexural Characteristics of Steel Fibre and Polyethylene Fibre Hybrid-Reinforced concrete. *Composites* 13, 164–168. doi:10.1016/0010-4361(82)90054-4

Li, Y., Yang, E., and Tan, K. (2020). Flexural Behavior of Ultra-high Performance Hybrid Fiber Reinforced concrete at the Ambient and Elevated Temperature. *Constr. Build. Mater.* 250, 118487. doi:10.1016/j.conbuildmat.2020.118487

Özkan, Ş., and Demir, F. (2020). The Hybrid Effects of PVA Fiber and basalt Fiber on Mechanical Performance of Cost Effective Hybrid Cementitious Composites. *Construction Building Mater.* 263, 120564. doi:10.1016/j.conbuildmat.2020.120564

Pan, Z., Wu, C., Liu, J., Wang, W., and Liu, J. (2015). Study on Mechanical Properties of Cost-Effective Polyvinyl Alcohol Engineered Cementitious Composites (PVA-ECC). *Construction Building Mater.* 78, 397–404. doi:10.1016/j.conbuildmat.2014.12.071

Park, S. H., Kim, D. J., Ryu, G. S., and Koh, K. T. (2012). Tensile Behavior of Ultra High Performance Hybrid Fiber Reinforced concrete. *Cement and Concrete Composites* 34 (2), 172–184. doi:10.1016/j.cemconcomp.2011.09.009

Rashiddadash, P., Ramezanianpour, A., and Mahdikhani, M. (2014). Experimental Investigation on Flexural Toughness of Hybrid Fiber Reinforced concrete (HFRC) Containing Metakaolin and Pumice. *Constr. Build. Mater.* 51, 313–320. doi:10.1016/j.conbuildmat.2013.10.087

Silva, E. R., Coelho, J. F. J., and Bordado, J. C. (2013). Strength Improvement of Mortar Composites Reinforced with Newly Hybrid-Blended Fibres: Influence of Fibres Geometry and Morphology. *Construction Building Mater.* 40, 473–480. doi:10.1016/j.conbuildmat.2012.11.017

Stahli, P., and Mier, J. (2007). Manufacturing, Fibre Anisotropy and Fracture of Hybrid Fibre concrete. *Eng. Fract. Mech.* 74, 223–242. doi:10.1016/j.engfracmech.2006.01.028

Standard for test methods of concrete physical and mechanical properties GB/T 50081-2019 (2019). Beijing, China: China Architecture and Building Press.

Technical specification for fiber reinforced concrete structures CECS (2004). Beijing, China: Planning Press.

Tian, H., Zhang, Y., Ye, L., and Yang, C. (2015). Mechanical Behaviours of green Hybrid Fibre-Reinforced Cementitious Composites. *Constr. Build. Mater.* 95, 152–163. doi:10.1016/j.conbuildmat.2015.07.143

Tran, T., Tran, N., and KIm, D. (2021). Enhancing Impact Resistance of Hybrid Ultra-high-performance Fiber-Reinforced Concretes through Strategic Use of Polyamide Fibers. *Constr. Build. Mater.* 271, 121562. doi:10.1016/j.conbuildmat.2020.121562

Turk, K., Bassurucu, M., and Bitkin, R. (2021). Workability, Strength and Flexural Toughness Properties of Hybrid Steel Fiber Reinforced SCC with High-Volume Fiber. *Constr. Build. Mater.* 266, 120944. doi:10.1016/j.conbuildmat.2020.120944

Yoo, D.-Y., Kim, M. J., Kim, S.-W., and Park, J.-J. (2017). Development of Cost Effective Ultra-high-performance Fiber-Reinforced concrete Using Single and Hybrid Steel Fibers. *Construction Building Mater.* 150, 383–394. doi:10.1016/j.conbuildmat.2017.06.018

Yoo, D.-Y., Sohn, H.-K., Borges, P. H. R., Fediuk, R., and Kim, S. (2020). Enhancing the Tensile Performance of Ultra-high-performance concrete through Strategic Use of Novel Half-Hooked Steel Fibers. *J. Mater. Res. Tech.* 9 (3), 2914–2925. doi:10.1016/j.jmrt.2020.01.042

Yoo, D., and Kim, M. (2019). High Energy Absorbent Ultra-high-performance concrete with Hybrid Steel and Polyethylene Fibers[J]. *Constr. Build. Mater.* 209, 354–363. doi:10.1016/j.conbuildmat.2019.03.096

Yoo, D., Kim, S., and Lee, S. (2018). Self-sensing Capability of Ultra-high-performance concrete Containing Steel Fibers and Carbon Nanotubes under Tension. *Sens. Actuators, A.* 276, 125–136. doi:10.1016/j.sna.2018.04.009

Yu, J., Zhang, H., and Qi, Y. (2021). Uniaxial Tensile Test and Numerical Simulation of Hybrid Fiber Reinforced concrete. *IOP Conf. Ser. Earth Environ. Sci.* 643, 012066. doi:10.1088/1755-1315/643/1/012066

Yu, K., McGee, W., Ng, T., Zhu, H., and Li, V. (2021). 3D-printable engineered cementitious composites (3DP-ECC): Fresh and hardened properties. *Cem. Concr. Res.* 143, 106388. doi:10.1016/j.cemconres.2021.106388

Zhao, J., Shi, H., and Lu, X. (2019). *Basic properties and test methods of ultra-high performance concrete*. Beijing: China: Building Materials Press.

Conflict of Interest: The authors declare that the research was conducted in the absence of any commercial or financial relationships that could be construed as a potential conflict of interest.

Publisher's Note: All claims expressed in this article are solely those of the authors and do not necessarily represent those of their affiliated organizations, or those of the publisher, the editors, and the reviewers. Any product that may be evaluated in this article, or claim that may be made by its manufacturer, is not guaranteed or endorsed by the publisher.